${}^{3}_{\Lambda}\mathrm{H}$ and ${}^{4}_{\Lambda}\mathrm{H}$ Lifetime, Yield, Directed Flow Measurements in Au+Au Collisions at $\sqrt{s_{NN}}$ = 3 GeV With the STAR Detector

Chenlu Hu[1,*] for STAR collaboration

[1]Quark Matter Research Center, Institute of Modern Physics, Chinese Academy of Sciences

Abstract. In this proceedings, the lifetime and yields of ${}^{3}_{\Lambda}\mathrm{H}$ and ${}^{4}_{\Lambda}\mathrm{H}$ in Au+Au collisions at $\sqrt{s_{NN}}$ = 3 GeV are presented. The measured yields are compared to measurements at other energies and theoretical models, and the physics implications are discussed. We also report the first observation of the ${}^{3}_{\Lambda}\mathrm{H}$ and ${}^{4}_{\Lambda}\mathrm{H}$ directed flow in 5 - 40% centrality. The directed flow of ${}^{3}_{\Lambda}\mathrm{H}$ and ${}^{4}_{\Lambda}\mathrm{H}$ are compared with those of the copiously produced particles such as p, Λ, d, t, ${}^{3}\mathrm{He}$, and ${}^{4}\mathrm{He}$. These results shed light on light hyper-nuclei production in heavy-ion collisions in the high baryon density region.

1 Introduction

As is known to all, the normal nucleus is made up of protons and neutrons. When a nucleon is replaced by a Λ hyperon ($S = -1$. Here S denotes the quantum number of strangeness), the nucleus is transformed into a hyper-nucleus which allows us to study the hyperon-nucleon (Y-N) interaction. It is well known that 2-body and 3-body Y-N interactions, especially at high baryon density, are essential for understanding the inner structure of compact stars [1-2]. Measurements of the lifetime, binding energy, decay branching ratios of hyper-nuclei can give us important information on Y-N interaction.

Anisotropic flow has been commonly used for studying the properties of matter created in high energy nuclear collisions, due to its genuine sensitivity on early stage collision dynamics [3]. The first order coefficient of the Fourier-expansion of azimuthal distribution, known as directed flow (v_1), has been analyzed for all particles ranging from the lightest pion-mesons to light nuclei in such collisions [4-5].

In this proceedings, the lifetime, yields and directed flow of ${}^{3}_{\Lambda}\mathrm{H}$ and ${}^{4}_{\Lambda}\mathrm{H}$ in Au+Au collisions at $\sqrt{s_{NN}}$ = 3 GeV will be discussed. The data was collected by the STAR experiment at RHIC with the fixed-target (FXT) setup. The gold beam of 3.85 GeV/u is collided on a thin gold target with 1% interaction probability, located at 200 cm along the beam direction from the center of the STAR Time-Projection Chamber (TPC). A total of 260M good minimum bias (MB) events were selected for this analysis.

2 Data Analysis, Results and Discussion

At the $\sqrt{s_{NN}}$ = 3 GeV collisions, the first order event plane is determined by the Event Plane Detector (EPD) [6], which is designed to measure the pattern of forward-going charged

*e-mail: huchenlu@impcas.ac.cn

particles emitted in heavy-ion collisions and covers a pseudorapidity range of $2.14 < |\eta| < 5.09$. The directed flow (v_1) discussed below is determined by the first order event plane.

2.1 Particle Reconstruction

The hyper-nuclei ${}^{3}_{\Lambda}$H and ${}^{4}_{\Lambda}$H are reconstructed with following decay channels: ${}^{3}_{\Lambda}\mathrm{H} \rightarrow {}^{3}\mathrm{He} + \pi^-$, ${}^{3}_{\Lambda}\mathrm{H} \rightarrow \mathrm{d} + \mathrm{p} + \pi^-$, ${}^{4}_{\Lambda}\mathrm{H} \rightarrow {}^{4}\mathrm{He} + \pi^-$. To assure the quality of each track, a minimum of 15 hits out of 45 hits in the TPC is required. The secondary decay topology is reconstructed by the KFParticle program which is based on a Kalman filter method [7]. In the program, the error-matrices are used to enhance the reconstruction significance. A set of cuts on topological variables are applied to the hyper-nuclei candidates to optimize the significance.

2.2 ${}^{3}_{\Lambda}$H and ${}^{4}_{\Lambda}$H Lifetime Measurements

The reconstructed ${}^{3}_{\Lambda}$H and ${}^{4}_{\Lambda}$H candidates are divided into different $L/\beta\gamma$ intervals, where L is is the decay length, β and γ are particle velocity and Lorentz factor, respectively. The raw signal counts N^{raw} for each $L/\beta\gamma$ interval are obtained from corresponding background-subtracted invariant mass spectrum using a bin counting method. The signal counts are corrected with the detector acceptance and reconstruction efficiency ($\varepsilon_{TPC} \times \varepsilon_{PID}$). The corrected hyper-nuclei counts as a function of $L/\beta\gamma$ is fitted to an exponential function ($N = N_0 e^{-L/\beta\gamma c\tau}$) to obtain the mean lifetime τ.

The lifetimes 232 ± 29(stat.) ± 37(syst.) for ${}^{3}_{\Lambda}$H (2-body decay channel) and 218 ± 8(stat.) ± 12(syst.) for ${}^{4}_{\Lambda}$H are obtained from the $\sqrt{s_{NN}} = 3$ GeV data. As shown in Fig. 1, the ${}^{4}_{\Lambda}$H measurement is the most precise measurement to date, and within uncertainties, the measured ${}^{3}_{\Lambda}$H and ${}^{4}_{\Lambda}$H lifetimes are consistent with previous measurements from ALICE [8, 9], STAR [10], HypHI [11].

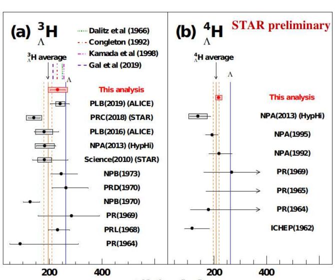

Figure 1. Measured lifetimes of ${}^{3}_{\Lambda}$H (a) and ${}^{4}_{\Lambda}$H (b) are shown comparing to previous measurements and theoretical calculations as well as the free Λ lifetime. The experimental average lifetimes and the corresponding uncertainty of ${}^{3}_{\Lambda}$H and ${}^{4}_{\Lambda}$H are also shown as orange bands.

2.3 ${}^{3}_{\Lambda}$H and ${}^{4}_{\Lambda}$H Yield Measurements

The hyper-nuclei ${}^{3}_{\Lambda}$H and ${}^{4}_{\Lambda}$H yields from their 2-body decay channels are extracted as a function of p_T and y in two centrality selections: 0–10% and 10–50%. The efficiency-corrected p_T spectra in each rapidity slice are extrapolated down to p_T=0 to obtain p_T integrated value of yields (dN/dy). Different functions (e.g blast-wave function) are used to estimate the systematic uncertainties in the unmeasured p_T regions. We have assumed branching ratios of 25% and 50% for the 2-body decay of ${}^{3}_{\Lambda}$H and ${}^{4}_{\Lambda}$H, respectively.

The ${}^{3}_{\Lambda}$H and ${}^{4}_{\Lambda}$H yields at $|y| < 0.5$ as a function of beam energy in central heavy-ion collisions are extracted and are compared to theoretical models as shown in Fig. 2. For ${}^{3}_{\Lambda}$H, the measured yield is consistent with the thermal model from GSI/Heidelberg [12]. The thermal model adopting the canonical ensemble can approximately describe the ${}^{3}_{\Lambda}$H yield both at 3 GeV and 2.76 TeV. Canonical ensemble thermal statistics is required to account for the large ϕ/K^- and ϕ/Ξ^- ratios measured at the same energy as well. We also observe that the coalescence model (DCM) [13] is consistent with the $^{3}_{\Lambda}$H yield while underestimating the $^{4}_{\Lambda}$H. On the other hand, the hybrid UrQMD overestimates both $^{3}_{\Lambda}$H and $^{4}_{\Lambda}$H yields by an order of magnitude.

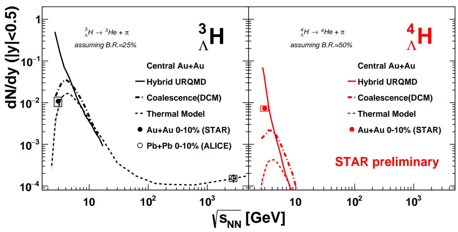

Figure 2. $^{3}_{\Lambda}$H (a) and $^{4}_{\Lambda}$H (b) yields at |y| < 0.5 as a function of beam energy in central heavy ion collisions. The symbols represent measurements while the lines represent different theoretical calculations. The data points assume a branching ratio of 25(50)% for $^{3}_{\Lambda}$H($^{4}_{\Lambda}$H) → ^{3}He(^{4}He) + π^-.

2.4 $^{3}_{\Lambda}$H and $^{4}_{\Lambda}$H Directed Flow Measurements

Directed flow of Λ hyperons, $^{3}_{\Lambda}$H, and $^{4}_{\Lambda}$H are extracted with event plane method. Figure 3 shows the v_1 for hyper-nuclei and Λ hyperons versus rapidity from the $\sqrt{s_{NN}}$ = 3 GeV Au + Au collisions. The yellow-red line is the result of linear fit to the data and is plotted in full rapidity region |y| ⩽ 0.9. For comparison, the v_1 distributions for p, d, t, ^{3}He and ^{4}He, from the events with same centrality, are shown as open symbols in the figure. Here the results of the linear fits to the light-nuclei are plotted as dashed-lines only in the positive rapidity region. As one can see, the v_1 of Λ hyperons is consistent with that of protons, and the slopes of hyper-nuclei v_1 are also similar to that of the corresponding light-nuclei with the same mass number within statistical uncertainties.

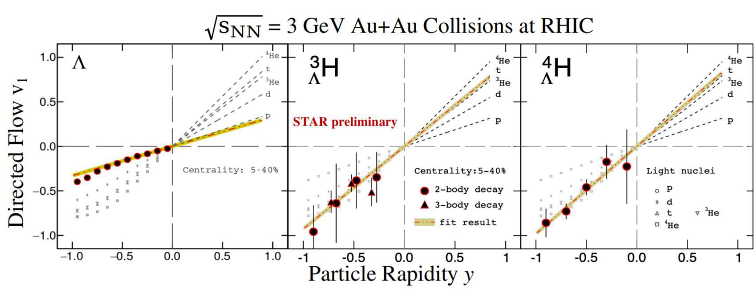

Figure 3. Hyper-nuclei v_1 as a function of rapidity from the $\sqrt{s_{NN}}$ = 3 GeV 5 − 40% mid-central Au + Au collisions at RHIC-STAR. In case of $^{3}_{\Lambda}$H, both 2-body (dots) and 3-body (triangles) decays are used. Results from fitting with a first-order polynomial function are shown as the yellow-red lines. The rapidity dependence of v_1 for p, d, t,^{3}He and ^{4}He are also shown as open-circles, diamonds, up-triangles, down-triangles and squares, respectively. The corresponding results of the linear fits are shown as dashed lines in the positive rapidity region.

Extracted mid-rapidity v_1 slopes, $dv_1/dy|_{y=0}$, for Λ hyperons, $^{3}_{\Lambda}$H, and $^{4}_{\Lambda}$H, are summarized in Fig. 4 as red filled-squares, as a function of particle mass. For comparison, the slopes of light-nuclei p, d, t, ^{3}He, and ^{4}He from the events with same centrality class (5-40%) in $\sqrt{s_{NN}}$ = 3 GeV Au+Au collisions are shown as open circles. The result of a linear fit to the light-nuclei is shown as the yellow-red line in the figure. Overall, hyper-nuclei v_1 slopes are consistent with that of light-nuclei which has similar mass albeit the large uncertainties in the results. The mass dependence of the v_1 slope implies that the coalescence is the dominant mechanism for hyper-nuclei production in heavy-ion collisions.

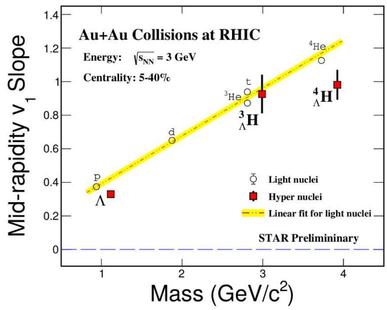

Figure 4. Mass dependence of the mid-rapidity v_1 slope $dv_1/dy|_{y=0}$ for Λ, $^3_\Lambda$H and $^4_\Lambda$H, from the $\sqrt{s_{NN}} = 3$ GeV mid-central 5-40% Au+Au collisions. Combined results of 2-body and 3-body decays are used for $^3_\Lambda$H while the $^4_\Lambda$H is only reconstructed from the 2-body decay. The slopes of light-nuclei p, d, t, ^{3}He and ^{4}He from the same collisions are shown as open circles. The yellow-red line is the result of a linear fit to the measured light nuclei v_1 slopes.

3 Summary

In summary, we reconstruct the light hyper-nuclei $^3_\Lambda$H and $^4_\Lambda$H from $\sqrt{s_{NN}} = 3$ GeV Au+Au collisions at RHIC-STAR. Lifetimes of $^3_\Lambda$H and $^4_\Lambda$H from their 2-body decay channel are measured to be 232 ± 29(stat.) ± 37(syst.) and 218 ± 8(stat.) ± 12(syst.) respectively. The $^3_\Lambda$H and $^4_\Lambda$H lifetimes are consistent with previous measurements and theoretical calculations. Meanwhile, the hyper-nuclei $^3_\Lambda$H and $^4_\Lambda$H yields at $|y| < 0.5$ as a function of beam energy in central heavy-ion collisions are reported and compared to theoretical models. We also reported the first observation of $^3_\Lambda$H and $^4_\Lambda$H directed flow v_1 from mid-central (5-40%) collisions. The rapidity dependence of their v_1 are compared with that of Λ hyperon and light nuclei p, d, t, ^{3}He and ^{4}He from the collisions with the same centrality class. It is found that, within statistical uncertainties, the mid-rapidity v_1 slope of $^3_\Lambda$H and $^4_\Lambda$H are similar to those of light nuclei with the similar mass, such as t, ^{3}He, and ^{4}He. In other words, they seem to follow the baryon mass scaling. These observations imply that coalescence of nucleons and Λ hyperons is the dominant mechanism for the light hyper-nuclei production in such collisions.

4 Acknowledgments

We thank Drs. Y. Nara and J. Steinheimer for interesting discussions and the use of simulations code of JAM and UrQMD.

References

[1] D. Gerstung, N. Kaiser, and W. Weise, Eur. Phys. J. **A56**, 175 (2020)
[2] D. Lonardoni et al., Phys. Rew. Lett. **114**, 092301 (2015)
[3] C.M. Hung and E. Shuryak, Phys. Rev. Lett. **75**, 4003 (1995)
[4] L. Adamczyk et al. (STAR Collaboration), Phys. Rev. Lett. **112**, 162301 (2014)
[5] M.S. Abdallah et al. (STAR Collaboration), Phys. Rev. **C103**, 034908 (2021)
[6] J. Adams et al. (STAR Collaboration), NIM **A968**, 163970 (2020)
[7] I. Kisel et al. (CBM Collaboration), J. Phys. Conf. Ser. **1070**, 012105 (2018)
[8] S. Acharya et al. (ALICE), Phys. Lett. B **797**, 134905 (2019), 1907.06906.
[9] J. Adam et al. (ALICE), Phys. Lett. B **754**, 360 (2016), 1506.08453.
[10] L. Adamczyk et al. (STAR), Phys. Lett. C **97**, 054909 (2018), 1710.00436.
[11] C. Rappold et al., Nucl. Phys. A **913**, 170 (2013), 1305.4871.
[12] A. Andronic, Phys. Lett. B **679**, 203 (2011), 1010.2995.
[13] J. Steinheimer, K. Gudima, A. Botvina, I. Mishustin, M. Bleicher, and H. Stocker, Phys. Lett. B **714**, 85 (2012), 1203.2547.